[CANCER RESEARCH 63, 2188–2193, May 1, 2003]

Overexpression of High Mobility Group Box 1 in Gastrointestinal Stromal Tumors with *KIT* Mutation[1]

Yon Rak Choi,[2] Hyunki Kim,[2] Hyun Ju Kang,[2] Nam-Gyun Kim, Jung Jin Kim, Kang-Sik Park, Young-Ki Paik, Hyun Ok Kim, and Hoguen Kim[3]

Department of Pathology [Y. R. C., Hy. K., H. J. K., N-G. K., J. J. K., Ho. K.], Brain Korea 21 Projects for Medical Sciences [Y. R. C., Hy. K., H. J. K.], Laboratory Medicine [H. O. K.], Yonsei Proteome Research Center [K-S. P., Y-K. P.], and Cancer Metastasis Research Center [N-G. K., Ho. K.], Yonsei University College of Medicine, 120-752 Seoul, Korea

ABSTRACT

Gain-of-function mutations of *KIT* are common genetic events in gastrointestinal stromal tumors (GISTs). To investigate the molecular characteristics of *KIT* mutations in GISTs, 20 GISTs (14 GISTs with *KIT* mutation and 6 GISTs without *KIT* mutation) were analyzed by two-dimensional electrophoresis and matrix-associated laser desorption ionization mass spectrophotometry-time of flight. Comparative analysis of the respective spot patterns on two-dimensional electrophoresis showed that HMGB1, an intranuclear protein that interacts with several transcription factors and plays a role in tumor metastasis after its secretion, was overexpressed in GISTs with *KIT* mutation. All of the 14 GISTs with *KIT* mutation, and only 2 of 6 GISTs without *KIT* mutation, revealed HMGB1 expression. Of the GISTs with *KIT* mutation, 12 (86%) showed strong expression of HMGB1, more than three times higher in intensity than the maximum observed in the 6 GISTs without *KIT* mutation by two-dimensional electrophoresis analysis. The overexpression of HMGB1 was further supported by Western blot analysis, and directly related to matrix metalloproteinase 2 overexpression. Our results indicate that the overexpression of HMGB1 is common in GISTs and is related to the *KIT* mutation, and that this may play a role in the tumorigenesis of GISTs because overexpressed HMGB1 could accelerate genes related to tumor growth and invasion.

INTRODUCTION

GISTs[4] are the most common mesenchymal tumors composed of uncommitted mesenchymal cells (1). Recent studies have described the morphological and immunohistochemical similarities between the ICCs and GISTs (2, 3). Immunohistochemically, tumor cells of GISTs characteristically express CD34 and KIT, ICCs are located in and near the circular muscle layer of the stomach and intestine, thus suggesting that GISTs originate from stem cells that differentiate toward ICCs.

Among the molecular genetic changes reported to be related to GISTs, gain-of-function mutations of the *KIT* proto-oncogene are the most frequent and important (3–5). *KIT* encodes a type III receptor kinase (6), the ligand of which is stem cell factor (7). Mutations in *KIT* result in ligand-independent kinase activity and autophosphorylation of KIT (8, 9). The *KIT* mutation is known to be present in 30–92% of GISTs (5, 10–12). Mutations are reported to be most frequent in exon 11 and rare in exons 9 and 13. Deletions, insertions, and point mutations have been reported, and mutations of exon 11 and exon 13 were reported to be gain-of-function mutations (3, 5, 11). Recent studies have also demonstrated that STI571, an inhibitor of tyrosine kinase, was effective at treating GISTs (13).

Although there is much experimental and clinical evidence that gain-of-function mutations of *KIT* evoke uncontrolled cell proliferation and stimulate downstream signaling pathways, the specific downstream pathways related to tumor development and/or progression of GISTs and the target molecules have not been elucidated. We, therefore, carried out a proteomic study on 20 GISTs and compared the results with respect to the *KIT* mutation status.

MATERIALS AND METHODS

Tissue Samples. Twenty GISTs of the stomach were included in this study. All of the cases were identified prospectively and consecutively in the Department of Pathology at Yonsei University Medical Center between September 1995 and November 2000 for molecular marker studies. Among these 20 cases, 14 had previously been analyzed for chromosomal changes (14). Information from hospital charts and clinicians was obtained on demographic features and tumor sites. The patients included 9 females and 11 males ranging in age from 35 to 79 years (Table 1). Thirteen colorectal carcinomas were also selected for comparison.

For DNA and protein extraction, fresh tumors and adjacent nontumorous smooth muscle or mucosal tissues were obtained immediately after surgical excision and were stored at −70° before use. To enrich the tumor cell population, areas with more than 90% of tumor cells were selected from H&E-stained slides using the cryostat microdissection technique. Genomic DNA was prepared using the SDS-proteinase K and phenol-chloroform extraction method.

Conventional pathological parameters (tumor size, number, differentiation) were examined prospectively without prior knowledge of the molecular data. The GISTs were divided into three groups according to the criteria of Lewin *et al.* (1). The guidelines for the diagnosis of gastric stromal tumor malignancy are composed of two unequivocal factors (histologically confirmed metastasis and invasion of adjacent organs) and seven high-risk factors (larger than 5.5 cm in diameter; more than five mitoses per 50 high power fields; presence of tumor necrosis; nuclear pleomorphism; dense cellularity; microscopic invasion into the lamina propria or blood vessels; and the presence of alveolar or cell balls). Tumors having more than one unequivocal or two high-risk features were categorized as malignant GISTs, tumors having only one high-risk feature were categorized as borderline GISTs, and tumors having neither unequivocal nor high-risk features were categorized as benign GISTs. According to these criteria, 4 cases were categorized as benign, 10 cases as borderline, and 6 cases as malignant GIST (Table 1).

***KIT* Mutation Analysis.** Somatic mutations in exons 9, 11, 13, and 17 of *KIT* were detected using PCR-based assay with previously described primers (5, 10, 11). PCR was carried out in a mixture of 20 μl containing 1.5 mM $MgCl_2$; 20 pmol of primer; 0.2 mM each dATP, dGTP, and dTTP; 5 μM dCTP; 1 μCi of [α-^{32}P]dCTP (3000 Ci/mmol; DuPont New England Nuclear, Boston, MA); 50 ng of sample DNA; 1× PCR buffer; and 1.25 units of Taq DNA polymerase (Life Technologies, Inc., Grand Island, NY). After denaturation at 95°C for 5 min, DNA amplification was performed for 25–30 cycles. Each cycle consisted of denaturation at 95°C for 30 s, primer annealing at 55°C for 30 s, and elongation at 72°C for 15 s. PCR products were separated in 6%

Received 7/24/02; accepted 3/5/03.

The costs of publication of this article were defrayed in part by the payment of page charges. This article must therefore be hereby marked *advertisement* in accordance with 18 U.S.C. Section 1734 solely to indicate this fact.

[1] Supported by grants of the 2001 Korean National Cancer Program, Ministry of Health and Welfare, Republic of Korea (to Ho. K.), Cancer Metastasis Research Center at Yonsei University (to Ho. K.), "21C Frontier Project: Functional Genomics of the Human Genome" (to Y-K. P., FG-1-4-01), and Adult Stem Cell No. 5 (to H. O. K.) from Stem Cell Research Center of the 21C Frontier Research Program funded by the Ministry of Science and Technology, Republic of Korea.

[2] Y. R. C., Hy. K., and H. J. K. contributed equally to this work.

[3] To whom requests for reprints should be addressed, at Department of Pathology, Yonsei University College of Medicine, CPO Box 8044, Seoul, Korea. Phone: 82-2-361-5263; Fax: 82-2-362-0860; E-mail: hkyonsei@yumc.yonsei.ac.kr.

[4] The abbreviations used are: GIST, gastrointestinal stromal tumor; KIT, v-kit Hardy-Zuckerman 4 feline sarcoma viral oncogene homologue; HMGB1, high mobility group box 1; MALDI-TOF, matrix-associated laser desorption ionization mass spectrophotometry-time of flight; MMP, matrix metalloproteinase; *p*I, isoelectric point; ICC, interstitial cell(s) of Cajal; ppm, parts per million.

Table 1 *Clinicopathological features, KIT mutation status, and HMGB1 expression levels of GISTs*

Sample no.	Tumor size (cm)	Tumor type	Anatomic site	Sex	Age	Comparative ratio of HMGB1 expression		Type of *KIT* mutation
						Western blot	2DE[a]	
1	1	Benign	Body	F	38	2.5	3.7	P551_V555del
2	2.5	Benign	Body	M	64	1.0	0.9	
3	4	Benign	Body	M	45	2.9	3.1	V559D
4	4	Benign	Body	F	36	3.7	3.3	M552_Y553del
5	7	Borderline	Body	M	52	2.2	3.1	W557R
6	5	Borderline	Antrum	F	47	0.1	0.2	
7	4	Borderline	Fundus	M	79	1.7	4.2	D579del
8	8	Borderline	Fundus	F	76	2.3	5.9	V560del
9	9	Borderline	Body	M	45	1.2	1.6	T574_R586ins
10	5.5	Borderline	Fundus	F	52	0.2	0.2	
11	17	Borderline	Fundus	F	64	2.7	3.8	D579del
12	5	Borderline	Body	F	56	0.7	0.1	
13	12	Borderline	Body	F	57	2.8	4.9	V559A
14	13	Borderline	Body	M	49	1.2	1.1	L576_R586ins
15	10	Malignant	Body	M	35	0.2	0.2	
16	17	Malignant	Body	M	78	1.0	1.0	
17	22	Malignant	Antrum	M	64	2.9	3.7	W557_K558del
18	3.7	Malignant	Fundus	M	44	2.3	5.0	K550_K558del
19	5.5	Malignant	Body	F	68	3.3	3.6	V559D
20	6	Malignant	Body	M	58	2.3	4.6	Y553_Q556del

[a] 2DE, two-dimensional electrophoresis; del, deletion; ins, insertion.

polyacrylamide gels, followed by autoradiography for single-strand conformational polymorphism analysis. The PCR products were also sequenced using an ABI Prism 310 Genetic Analyzer (Applied Biosystems, Foster City, CA).

Two-Dimensional Electrophoresis. GIST tissues were suspended in sample buffer containing 40 mM Tris, 7 M urea, 2 M thiourea, 4% 3-[(3-Cholamidopropyl)dimethylammonio]-1-propane sulfonate (CHAPS), 100 mM 1,4-dithioerythritol, and protease inhibitor cocktail (Roche, Mannheim, Germany). Suspensions were sonicated for ~30 s and centrifuged at 100,000 × *g* for 45 min. One mg of total GIST protein was used for each electrophoresis. Aliquots of proteins in sample buffer were applied onto immobilized pH 3–10 nonlinear gradient strips (Amersham Pharmacia Biotech, Uppsala, Sweden). Isoelectric focusing was conducted at 80,000 Vh. The second-dimension electrophoresis was carried out in 9–16% linear gradient polyacrylamide gels (18 cm × 20 cm × 1.5 mm) as described previously (15). After protein fixation in 40% methanol and 5% phosphoric acid for 12 h, gels were stained with Coomassie Blue G250 for 24 h. Gels were destained with H_2O and scanned in a Bio-Rad G710 densitometer, and data were converted into electronic files, which were then analyzed with Melanie III computer software (GenBio, Geneva, Switzerland).

Identification of Protein Spots. For mass spectrometry fingerprinting, protein spots were directly cut out of the gels, destained, and treated with trypsin. Aliquots of the peptide mixtures obtained from trypsin treatment were applied onto a target disk and allowed to air-dry. Spectra were obtained using a Voyager DE PRO MALDI-TOF spectrometer (Applied Biosystems, Foster City, CA). Protein database searching was performed with MS-Fit[5] using monoisotopic peaks. A mass tolerance was first allowed within 50 ppm, and then recalibration was performed at 20 ppm after obtaining the protein lists.

Western Blot Analysis. For Western blot analysis, tumor tissues and matched nontumorous smooth muscle tissues were suspended in ice-cold lysis buffer [50 mM Tris (pH 7.4), 1% Triton X-100, 5 mM EDTA, 1 mM KCl, 140 mM NaCl, 2 mM MgCl2, 1 mM phenylmethylsulfonyl fluoride, 1 mM sodium fluoride, 1% aprotinin, 1 uM leupeptin, and 1 mM sodium orthovanadate] for 15 min. Suspensions were sonicated for ~30 s and centrifuged at 20,000 × *g* for 15 min. For nuclear and cytoplasmic protein fractionation, five GISTs (three GISTs with *KIT* mutation and two GISTs without *KIT* mutation) that had sufficient amounts of tissue for preparation of tissue lysates were selected. Nuclear and cytoplasmic extracts were prepared as described previously (16, 17). Approximately 0.3 g of frozen tissue was added to a cryogenic vial containing 1 ml of buffer A [10 mM HEPES (pH 7.9), 10 mM KCl, 0.1 mM EDTA, 0.1 mM EGTA, 1 mM DTT, and 0.5 mM phenylmethylsulfonyl fluoride], and homogenized. The cells were allowed to swell on ice for 15 min, after which 50 μl of 10% NP40 were added. After vigorous vortexing for 10 s, the homogenate was centrifuged for 30 s. The supernatant was collected and used for cytoplasmic protein assay. The pellet was resuspended in 100 μl of ice-cold buffer C [20 mM HEPES (pH 7.9), 0.4 M NaCl, 1 mM EDTA, 1 mM EGTA, 1 mM DTT, and 1 mM phenylmethylsulfonyl fluoride] and shaken at 4°C for 15 min on a shaking platform. After being centrifuged for 5 min at 4°C, the supernatant was collected and used for nuclear protein assay. Twenty μg of total protein lysates and cytoplasmic extracts and 5 μg of nuclear protein extracts were loaded into each lane, size-fractionated by SDS-PAGE, and transferred to a polyvinylidene difluoride membranes that were blocked with Tris-buffered saline-Tween 20 containing 5% skim milk. Primary antibodies, KIT (C-19, polyclonal; Santa Cruz Biotech, Santa Cruz, CA), HMGB1 (polyclonal; BD Biosciences, Franklin Lakes, NJ), MMP2 (42–5D11, monoclonal; Calbiochem, Temecula, CA), glyceraldehyde-3-phosphate dehydrogenase (G3PDH; polyclonal; Trevigen, Gaithersburg, MD) were diluted 1:5000 in blocking buffer and incubated for 1 h at room temperature. After washing, membranes were incubated for 1 h with horseradish peroxidase-conjugated secondary antibody (Amersham Pharmacia Biotech), washed, and then developed with ECL-Plus (Amersham Pharmacia Biotech).

Immunohistochemical Analysis. Formalin-fixed and paraffin-embedded tissues were used for the immunostaining of KIT and HMGB1. Deparaffinization and rehydration were performed using xylene and alcohol. The sections were treated with 0.3% hydrogen peroxidase for 3 min and with blocking antibody for 30 min. The same primary antibodies used for Western blotting were applied in immunohistochemistry. The antibody against KIT protein was applied at 1:1000 (v/v), whereas the antibody against HMGB1 was at 1:100 (v/v). Avidin-biotin complex methodology was used. The chromogen was diaminobenzidine, and counterstaining was done with methyl green. The evaluation of KIT was categorized as expressed and absent. The expression of HMGB1 was categorized as overexpressed and normal. Cases with definite nuclear staining in more than 30% of the tumor cells and/or cytoplasmic expression were categorized as overexpressed, and cases with definite nuclear staining in less than 30% of the tumor cells were categorized as normal.

RESULTS

Mutation Status of *KIT*. *KIT* mutations were found in 14 of 20 tumors. All of the mutations were present in exon 11. No mutations were found in exons 9, 13, or 17. Deletion mutations were most frequent and were found in eight cases, whereas point mutations were found in four cases and insertions in two cases. Large deletions were present between codons 550 and 558, and single amino acid deletions were present at codons 560 and 579. The point mutations found were V557R, V559D, and V559A, which have been previously reported in GISTs.

[5] Internet address: http://prospector.ucsf.edu/ucsfhtml3.4/msfit.htm.

Two-Dimensional Electrophoresis Analysis of GISTs. Proteome analysis was performed on GISTs by high-resolution two-dimensional electrophoresis. More than 1000 protein spots were detected on the two-dimensional electrophoresis gels and localized in the ranges of *p*I 3–10 and a relative molecular mass of 10–200 kDa. We were able to identify more than 250 protein species in two-dimensional electrophoresis gels using MALDI-TOF spectrometry. Because matched normal tissues with the same histogenetic origin cannot be obtained in GISTs, we performed computer-assisted comparative analysis of the respective Coomassie Blue spot patterns of GISTs with and without *KIT* mutation or of benign and malignant GISTs. Accordingly, we found that HMGB1 [formerly named HMG1 (Ref. 18; Fig. 1*A*] was overexpressed in GISTs with *KIT* mutation.

Identification of HMGB1 as a Tumor Marker of GISTs with *KIT* Mutation. We focused on the expression of HMGB1 because some of the reported functions of HMGB1 are related to tumor growth and metastasis. Both the *p*I and the relative molecular mass of HMGB1 in each two-dimensional electrophoresis gel were determined by comparison with standard two-dimensional electrophoresis gels from the Swiss-Two-Dimensional-PAGE database. As shown in Fig. 1*B*, HMGB1 was overexpressed in GISTs with *KIT* mutation compared with the GISTs without *KIT* mutation. The relative expression level of HMGB1 in all 20 of the samples analyzed by two-dimensional electrophoresis was quantified using Melanie III computer software (GenBio). In the 14 GISTs with *KIT* mutation, all of the cases showed HMGB1 expression and 12 (86%) showed strong expression level, more than three times higher in intensity than the maximum observed in the six GISTs without *KIT* mutation (case 16). In the six GISTs without *KIT* mutation, four cases showed no detectable HMGB1 expression, and the remaining two cases showed weak expression. The expression of HMGB1 in colorectal carcinomas and matched normal mucosae was ubiquitous; however, marked variations were found. Of the 13 colorectal carcinomas, all of the tumors and matched normal mucosae showed detectable HMGB1 expression, and seven tumors showed more than three times higher intensity than the matched normal mucosae. Comparison of HMGB1 expression by volume percentage showed higher level expression in colorectal carcinomas and GISTs than in the nontumorous colon mucosae; the average volume percentage was 0.23 ± 0.19 for GISTs, 0.31 ± 0.14 for colorectal carcinomas, and 0.08 ± 0.06 for nontumorous colon mucosae. To further examine the molecular characteristics of HMGB1, the HMBG1 spot in two-dimensional electrophoresis was

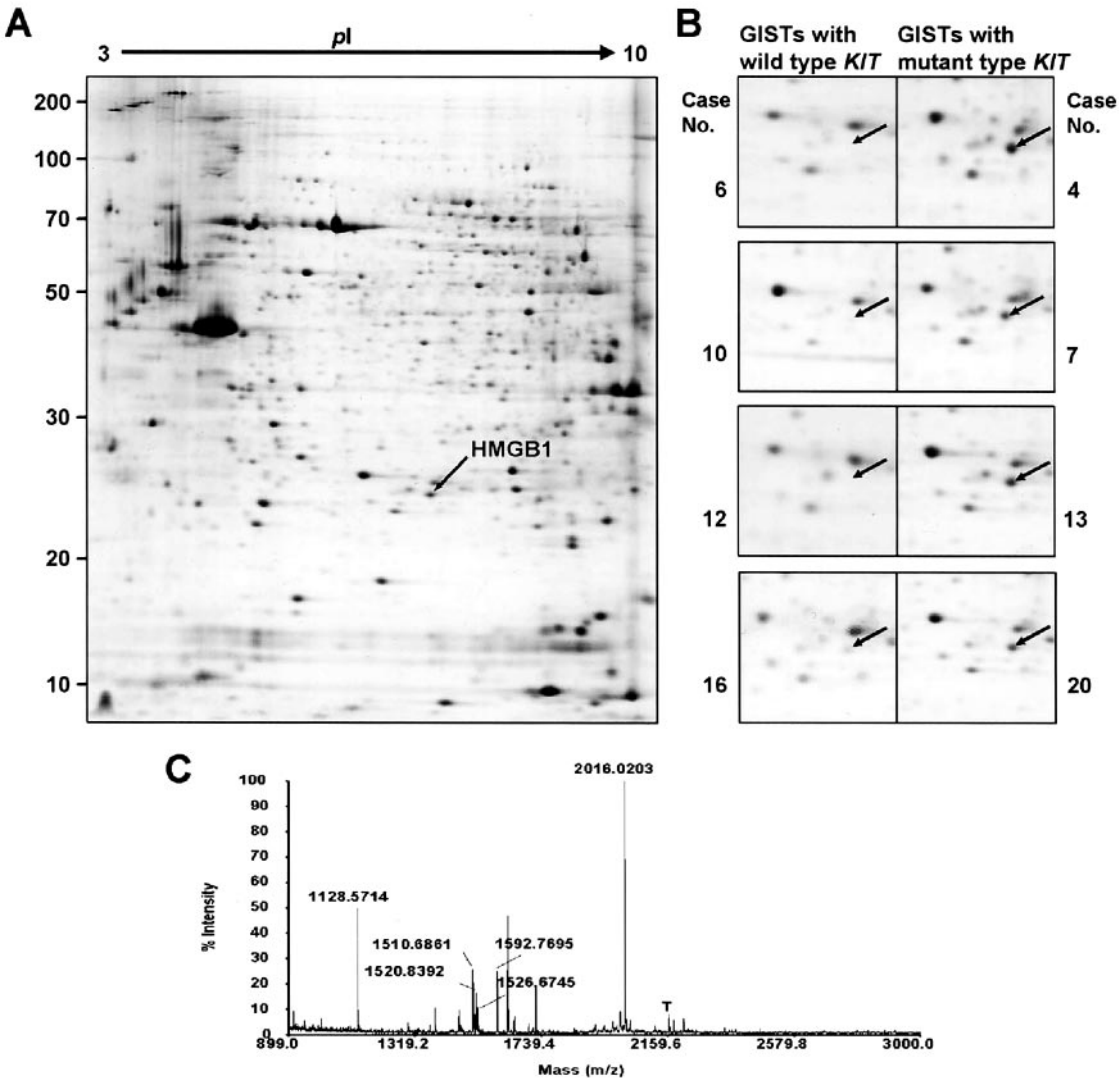

Fig. 1. Two-dimensional electrophoresis of HMGB1. *A*, two-dimensional electrophoresis of GIST tissue (case 13). The proteins from GIST were extracted and separated on pH 3–10 nonlinear immobilized pH-gradient strips and were run through a 9–16% SDS/polyacrylamide gel. The gel was stained with Coomassie Blue G250, and protein spots were examined by MALDI-TOF. *B*, two-dimensional electrophoresis gel images of HMGB1. Eight representative tissues of 20 cases are shown. *Arrows*, the protein spot corresponding to HMGB1. *C*, MALDI-TOF peptide mass spectrum of the tryptic digest of HMGB1; *T*, trypsin autolytic fragments.

Table 2 *Summary of MALDI-TOF masses obtained from tryptic digests of human HMGB1*[a]

Masses submitted	Monoprotonated masses matched	Delta ppm	Start	End	Proposed peptide sequence
1128.5714	1128.5689	2.1	155	163	(K) YEKDIAAYR(A)
1510.6861	1510.6823	2.5	13	24	(K) MSSYAFFVQTCR(E)
1520.8392	1520.8437	−2.9	113	127	(K) IKGEHPGLSIGDVAK(K)
1526.6745	1526.6772	−1.7	13	24	(K) MSSYAFFVQTCR(E)
1592.7695	1592.7709	−0.9	30	43	(K) KHPDASVNFSEFSK(K)
1592.7695	1592.7709	−0.9	31	44	(K) HPDASVNFSEFSKK(C)
1592.7695	1592.7379	19.9	128	141	(K) KLGEMWNNTAADDK(Q)
2016.0203	2016.0166	1.8	97	112	(K) RPPSAFFLFCSEYRPK(I)

[a] A total of 37% sequence coverage.

isolated and subjected to trypsin digestion followed by MALDI-TOF analysis. HMGB1 was validated by mass fingerprinting of the selected peaks of peptides by applying low tolerance (<20 ppm) with recalibration (Fig. 1*C*). For HMGB1, a total of six peaks were detected with 37% coverage (Table 2). This information led us to believe that the proteins detected in 20 samples by two-dimensional electrophoresis were authentic HMGB1. These HMGB1 spots on two-dimensional electrophoresis also showed the expected mass profiles that were well matched with the theoretical values of HMGB1.

Western Blot and Immunohistochemical Analysis for KIT and HMGB1. To determine the relative protein expression levels of both KIT and HMGB1, in which the former was not detectable in two-dimensional electrophoresis under the same conditions, Western blot analysis was carried out using antibodies against KIT and HMGB1 (Fig. 2). KIT expression was strong in GISTs with *KIT* mutation, and this overexpression was directly related to mutation, regardless of the mutation type. The relative expression ratio of KIT was 3.6 in cases with *KIT* mutation and 0.5 in cases without *KIT* mutation. As expected, HMGB1 was found to be consistently overexpressed in GISTs with *KIT* mutation. In accordance with the two-dimensional electrophoresis results, 11 of 14 GISTs with *KIT* mutation showed more than a 2-fold overexpression of HMGB1 compared with the maximally expressed HMGB1 level in those without *KIT* mutation (case 16). To determine whether the overexpression of HMGB1 is related to MMP expression, we performed Western analyses for MMP2 and found that all 12 of the cases with HMGB1 overexpression also strongly expressed MMP2 (Fig. 2). This result is consistent with the previous report by Taguchi *et al.* (19), in which secreted HMGB1 was found to induce MMP expression. The results of Western blot analysis for HMGB1 expression in colorectal carcinomas were also correlated with the results of the two-dimensional electrophoresis. HMGB1 expression was found in most of the normal mucosae and tumors, and overexpression was noted in 10 of 13 tumors. The nuclear and cytoplasmic expression of HMGB1 was separately measured in five GISTs (three GISTs with *KIT* mutation and two without *KIT* mutation) by using fractionated nuclear and cytoplasmic protein lysates. All three of the GISTs with *KIT* mutation showed variable amounts of HMGB1 expression in the nuclear and cytoplasmic proteins, whereas weak or undetectable cytoplasmic expression was found in the two GISTs without *KIT* mutation, and one GIST without *KIT* mutation also showed no detectable nuclear HMGB1 expression (Fig. 3). Interestingly, KIT expression was correlated to the cytoplasmic expression level of HMGB1 and MMP2 (Fig. 3). Immunohistochemically, HMGB1 was detected mainly in the nuclei of the tumor cells, cytoplasms of some tumor cells, and some nuclei of the normal cells (Fig. 4). In 14 GISTs with *KIT* mutation, 12 showed nuclear HMGB1 expression, and 4 showed cytoplasmic HMGB1 expression. In six GISTs without *KIT* mutation, two showed nuclear HMGB1 expression and one showed cytoplasmic HMGB1 expression. In the colorectal carcinomas, stronger HMGB1 expression compared with that of the normal mucosal cells was found in most of the tumor cells; however, the level of expression between tumors was variable.

DISCUSSION

In this study, 20 GISTs were investigated for the mutation status of *KIT* and the characteristics of their protein expression. We found frequent mutations in exon 11 of *KIT* in our GISTs, and strong expression of KIT and HMGB1 in cases with *KIT* mutation.

Frequent mutations of *KIT* in GISTs had been reported by many laboratories (3, 5, 10, 11). In agreement with the previous reports, we found frequent mutations (14 of 20, 70%) in our GISTs. Most of the mutations were deletions (8 of 14, 57%) in exon 11, as has been previously reported. Exon 11 constitutes the juxtamembrane region of *KIT*, which serves as an antidimerization domain. Deletions, insertions, or point mutations in this domain result in the activation of tyrosine kinase activity by allowing ligand-independent receptor dimerization (8, 9). Recently germ-line and somatic point mutations of exon 13 (K642E) were reported and were found to be activating mutations in the kinase domain of *KIT* gene (11). In this study, we provide direct evidence of KIT protein overexpression in all of our GISTs with *KIT* mutation. KIT overexpression in GISTs is a well-

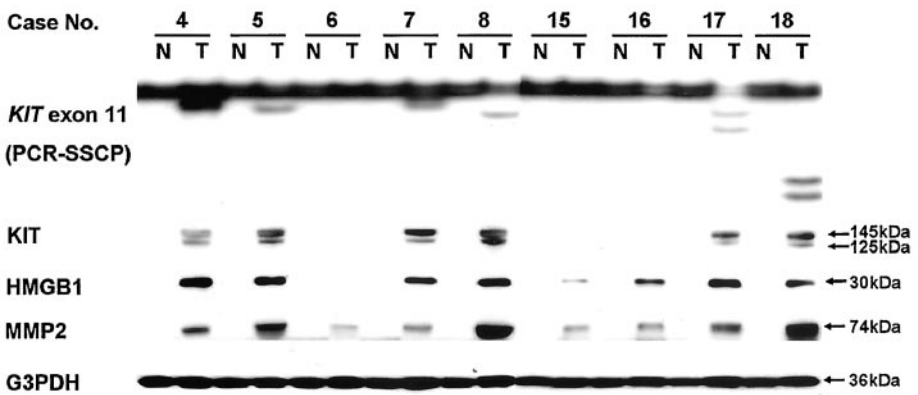

Fig. 2. Mutation of *KIT* exon 11 by PCR-single-strand conformational polymorphism analysis, and protein expression of KIT, HMGB1, and MMP2 in nine GIST tissues and matched normal smooth muscle tissues by Western blot analysis. Case 4 was benign, cases 5–8 were borderline, and cases 15–18 were malignant GISTs. Immunoblotting with KIT, HMGB1, and MMP2 antibodies after SDS-PAGE was performed as described in "Materials and Methods." Glyceraldehyde-3-phosphate dehydrogenase (*G3PDH*) was used as the reference for comparisons between normal gastrointestinal smooth muscle tissue and GIST. *N*, normal smooth muscle tissue; *T*, GIST tissue. *kDa*, M_r in thousands.

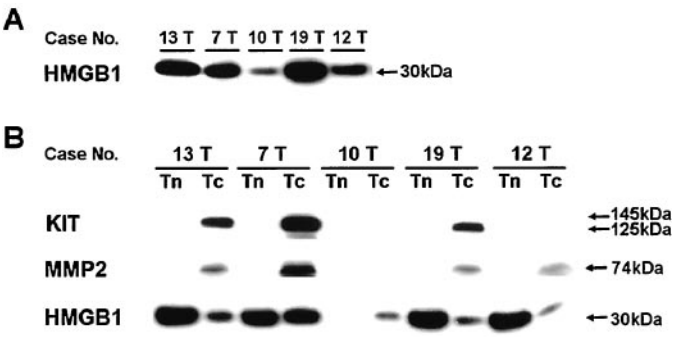

Fig. 3. Analysis of HMGB1 expression in nuclear and cytoplasmic proteins. *A*, HMGB1 expression in total protein lysates of five GISTs. Cases 13T, 7T, and 19T were positive for *KIT* mutation and cases 10T and 12T had no *KIT* mutation. *B*, analysis of HMGB1, KIT, and MMP2 expression in the nuclear and cytoplasmic protein fraction of five GISTs. Preparation of total protein lysates, nuclear protein fraction, and cytoplasmic protein fraction was performed as described in "Materials and Methods." *Tn*, nuclear protein lysates from GIST tissue; *Tc*, cytoplasmic protein lysates from GIST tissue. *kDa*, M_r in thousands.

known characteristic, and is currently used as a diagnostic marker. Most of the previous studies regarding KIT expression in GISTs in human tissues were performed by using immunohistochemistry, and quantitative evaluations of KIT expression and comparisons between this and *KIT* mutations has not been performed. We applied Western blot by using fresh tumor samples, thus enabling relative quantification by Western blot, and we compared the results with *KIT* mutation data. We found that KIT overexpression was directly related to *KIT* mutation regardless of the mutation type. The ubiquitous KIT activation in GISTs by activating *KIT* mutation (12) and its roles have previously been suggested epidemiologically (10, 12, 20). In addition, there have been a number of reports on the aberrant expression of KIT in other tumors (21–23) and on the relationship between *KIT* activation and the protection of apoptosis and the enhancement of tumor invasion (24). On the basis of these reports, we suggest that mutations of exon 11 of *KIT* induce the overexpression and the constitutive activation of KIT, which subsequently plays a role in tumor transformation and progression.

Initially, this work was designed as part of our attempts to identify a set of protein biomarkers involved in the progression of malignant tumors by proteome analysis. We used GISTs for the following reasons: (*a*) there are well-defined diagnostic criteria for differentiating benign, borderline, and malignant tumors; (*b*) most GISTs show similar chromosomal, morphological, and immunohistochemical characteristics; and (*c*) there are high percentages of tumor cells in GIST. During the course of this work, we found that several proteins are overexpressed in GISTs with *KIT* mutation, and, thus, we focused on the cause and consequence of HMGB1 overexpression in GISTs with *KIT* mutation. The implications of our proteome analysis are at least 3-fold. The direct link between *KIT* mutation and HMGB1 expression should be regarded as a novel finding. We found HMGB1 expression in all 14 of the GISTs with *KIT* mutation, and 12 of these showed very strong expression by two-dimensional electrophoresis analysis. In GISTs without *KIT* mutation, HMGB1 was not expressed in four of six GISTs. Interestingly, two GISTs with insertion mutations in the distal portion of exon 11 of *KIT* showed low levels of HMGB1 expression. From these results, we suspect that the constitutive activity of KIT caused by these two insertion mutations in the distal portion of exon 11 would be milder than that caused by mutations in the proximal portion of the juxtamembrane domain. Although the number of inserted sequences is not identical to ours, similar insertional mutations at the same sites have been reported previously (12), and further functional study of these two insertion mutations is needed.

We demonstrated that the tumor cells are the origin of overexpressed HMGB1 in our GISTs by immunohistochemical analysis. HMGB1 was abundantly expressed in the nuclei of the tumor cells and/or some of the tumor cell cytoplasms, and the expression was correlated with the result of two-dimensional electrophoresis and Western blot analysis. We also demonstrated marked variation of HMGB1 expression in colorectal carcinomas. Variations in HMGB1 expression at the RNA level had been reported in breast carcinomas (25), gastric carcinomas (26), and hepatocellular carcinomas (27). Overexpression of HMGB1 and cisplatin resistance had been reported (28), and the role of HMGB1 in the repair of cisplatin-DNA adduct had been proposed (28, 29). The marked intertumoral variation of HMGB1 expression level and the reported roles of HMGB1 in tissue differentiation and tumor progression raise the possibility that the roles of HMGB1 in tumor differentiation and progression may be different according to the HMGB1 expression level.

One of the important roles of the *KIT* mutation of GISTs in tumorigenesis may be the activation of signal transduction pathways of the cell cycle. In this study, we found that KIT, HMGB1, and MMP2 are concomitantly overexpressed in GISTs with *KIT* mutation, and, thus, HMGB1 and MMP2 may be downstream target molecules in GISTs with *KIT* mutation. HMGB1 was originally identified as a chromosomal DNA-binding protein (30). Apart from this intranuclear function, HMGB1 was also shown to be localized in the extracellular medium of different cell types as matrix-bound and in soluble molecules (31) and to have an extracellular function in inflammation and tumor metastasis (19, 32, 33). On the basis of the reported function of HMGB1, the role of HMGB1 overexpression in GIST tumorigenesis

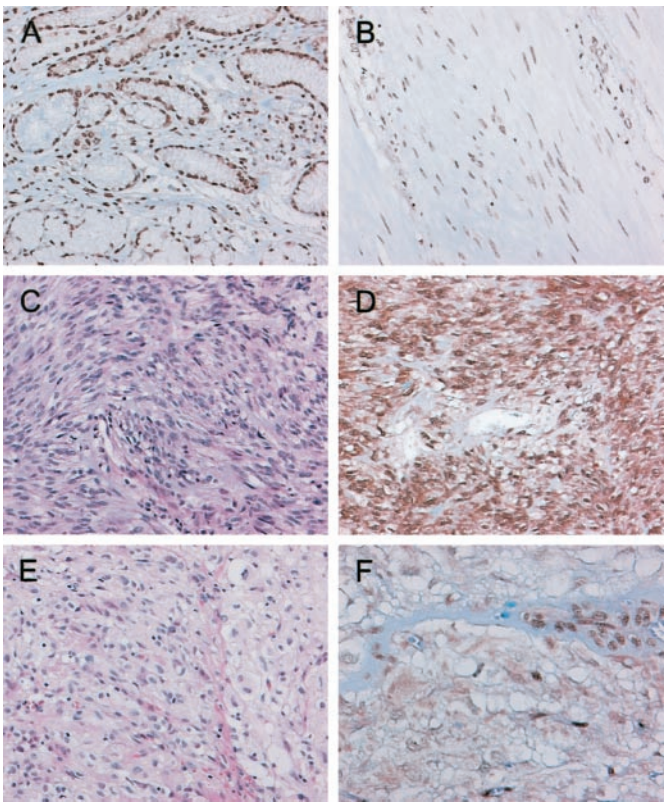

Fig. 4. Immunohistochemical analysis of HMGB1 in GISTs. Expression of HMGB1 is noted in the nuclei of epithelial cells and inflammatory cells in the gastric mucosa (*A*) and in the nuclei of smooth muscle cells (*B*). Microscopic feature of a GIST with *KIT* mutation (*C*), which shows strong nuclear and cytoplasmic HMGB1 expression (*D*). Histology of a GIST without *KIT* mutation (*E*) showing no HMGB1 expression in tumor cells. HMGB1 expression is evident only in the nuclei of the vascular smooth muscle cells and capillary endothelial cells (*F*).

can be explained in two ways. First, overexpressed HMGB1 can influence the expression and function of several related genes. HMGB1 is mainly localized in the nucleus and interacts with several transcription factors, by binding to the minor groove of DNA (33), increasing the binding affinity of several transcription factors, (34) and down-regulating the binding affinity of p53 and p73 in the human *BAX* promoter (35). Thus, we suggest that the overexpression of HMGB1 can contribute to tumorigenesis by altering tumor suppressor gene function. Second, HMGB1 directly activates signal transduction pathways related to cellular proliferation and/or metastasis. In addition to its intracellular role, HMGB1 is also secreted and/or released by certain cells and plays important roles in tumor growth, invasion, and metastasis (19, 33). Secreted and/or released HMGB1 binds to receptor for advanced glycation end products (RAGE), as a receptor-ligand pair, and this complex activates several molecules, including mitogen-activated protein kinase (MAPK) signaling molecules and MMPs. The suppression of tumor growth and metastasis by blocking RAGE-amphoterin (synonym of HMGB1) complex in mice had been reported (19). Therefore, it is likely that, after necrosis some of the overexpressed HMGB1 may exist in secreted forms or released forms that are capable of facilitating tumor growth and metastasis. Although we could not confirm that a portion of the HMGB1 in our GISTs was in a secreted form, we demonstrated the presence of HMGB1 by showing that MMP2 is selectively overexpressed according to HMGB1 expression in our GISTs. Taken together, our results suggest that *KIT* mutation in GISTs is strongly related to HMGB1 overexpression which may contribute to tumor growth and invasion.

REFERENCES

1. Lewin, K. J., Riddel, R. H., and Weinstein, W. M. Mesenchymal tumors. *In:* K. J. Lewin, R. H. Riddel and W. M. Weinstein (eds.), Gastrointestinal Pathology, pp. 284–341. Tokyo: Ikaku-Sroin, 1992.
2. Kindblom, L. G., Remotti, H. E., Aldenborg, F., and Meis-Kindblom, J. M. Gastrointestinal pacemaker cell tumor (GIPACT): gastrointestinal stromal tumors show phenotypic characteristics of the interstitial cells of Cajal. Am. J. Pathol., *152:* 1259–1269, 1998.
3. Hirota, S., Isozaki, K., Moriyama, Y., Hashimoto, K., Nishida, T., Ishiguro, S., Kawano, K., Hanada, M., Kurata, A., Takeda, M., Tunio, G. M., Matsuzawa, Y., Kanakura, Y., Shinomura, Y., and Kitamura, Y. Gain-of-function mutations of *c-kit* in human gastrointestinal stromal tumors. Science (Wash. DC), *279:* 577–580, 1998.
4. Nakahara, M., Isozaki, K., Hirota, S., Miyagawa, J., Hase-Sawada, N., Taniguchi, M., Nishida, T., Kanayama, S., Kitamura, Y., Shinomura, Y., and Matsuzawa, Y. A novel gain-of-function mutation of *c-kit* gene in gastrointestinal stromal tumors. Gastroenterology, *115:* 1090–1095, 1998.
5. Lasota, J., Jasinski, M., Sarlomo-Rikala, M., and Miettinen, M. Mutations in exon 11 of *c-Kit* occur preferentially in malignant *versus* benign gastrointestinal stromal tumors and do not occur in leiomyomas or leiomyosarcomas. Am. J. Pathol., *154:* 53–60, 1999.
6. Besmer, P., Murphy, J. E., George, P. C., Qiu, F. H., Bergold, P. J., Lederman, L., Snyder, H. W., Jr., Broudeur, D., Zuckerman, E. E., and Hardy, W. D. A new acute transforming feline retrovirus and relationship of its oncogene *v-kit* with the protein kinase gene family. Nature (Lond.), *320:* 415–421, 1986.
7. Williams, D. E., Eisenman, J., Baird, A., Rauch, C., Van, Ness, K., March, C. J., Park, L. S., Martin, U., Mochizuki, D. Y., and Boswell, H. S. Identification of a ligand for the *c-kit* proto-oncogene. Cell, *63:* 167–174, 1990.
8. Ma, Y., Cunningham, M. E., Wang, X., Ghosh, I., Regan, L., and Longley, B. J. Inhibition of spontaneous receptor phosphorylation by residues in a putative α-helix in the KIT intracellular juxtamembrane region. J. Biol. Chem., *274:* 13399–13402, 1999.
9. Kitayama, H., Kanakura, Y., Furitsu, T., Tsujimura, T., Oritani, K., Ikeda, H., Sugahara, H., Mitsui, H., Kanayama, Y., and Kitamura, Y. Constitutively activating mutations of *c-kit* receptor tyrosine kinase confer factor-independent growth and tumorigenicity of factor-dependent hematopoietic cell lines. Blood, *85:* 790–798, 1995.
10. Taniguchi, M., Nishida, T., Hirota, S., Isozaki, K., Ito, T., Nomura, T., Matsuda, H., and Kitamura, Y. Effect of *c-kit* mutation on prognosis of gastrointestinal stromal tumors. Cancer Res., *59:* 4297–4300, 1999.
11. Lux, M. L., Rubin, B. P., Biase, T. L., Chen, C-J., Maclure, T., Demetri, G., Xiao, S., Singer, S., Fletcher, C. D. M., and Fletcher, J. A. *KIT* extracellular and kinase domain mutations in gastrointestinal stromal tumors. Am. J. Pathol., *156:* 791–795, 2000.
12. Rubin, B. P., Singer, S., Tsao, C., Duensing, A., Lux, M. L., Ruiz, R., Hibbard, M. K., Chen, C. J., Xiao, S., Tuveson, D. A., Demetri, G. D., Fletcher, C. D., and Fletcher, J. A. KIT activation is a ubiquitous feature of gastrointestinal stromal tumors. Cancer Res., *61:* 8118–8121, 2001.
13. Joensuu, H., Roberts, P. J., Sarlomo-Rikala, M., Andersson, L. C., Tervahartiala, P., Tuveson, D., Silberman, S. L., Capdeville, R., Dimitrijevic, S., Druker, B., and Demetri, G. D. Effect of the tyrosine kinase inhibitor STI571 in a patient with a metastatic gastrointestinal stromal tumor. N. Engl. J. Med., *344:* 1052–1056, 2001.
14. Kim, N. G., Kim, J. J., Ahn, J. Y., Seong, C. M., Noh, S. H., Kim, C. B., Min, J. S., and Kim, H. Putative chromosomal deletions on 9p, 9q and 22q occur preferentially in malignant gastrointestinal stromal tumors. Int. J. Cancer, *85:* 633–638, 2000.
15. Park, K. S., Kim, H., Kim, N. G., Cho, S. Y., Choi, K. H., Seong, J. K., and Paik, Y. K. Proteomic analysis and molecular characterization of tissue ferritin light chain in hepatocellular carcinoma. Hepatology, *35:* 1459–1466, 2002.
16. Schreiber, E., Matthias, P., Muller, M. M., and Schaffner, W. Rapid detection of octamer binding proteins with 'mini-extracts', prepared from a small number of cells. Nucleic Acids Res., *17:* 6419, 1989.
17. Kim, H., Piao, Z., Kim, J. W., Choi, J. S., Kim, N. K., Lee, J. M., and Park, J. H. Expression of hMSH2 and hMLH1 in colorectal carcinomas with microsatellite instability. Pathol. Res. Pract., *194:* 3–9, 1998.
18. Bustin, M. Revised nomenclature for high mobility group (HMG) chromosomal proteins. Trends Biochem. Sci., *26:* 152–153, 2001.
19. Taguchi, A., Blood, D. C., del Toro, G., Canet, A., Lee, D. C., Qu, W., Tanji, N., Lu, Y., Lalla, E., Fu, C., Hofmann, M. A., Kislinger, T., Ingram, M., Lu, A., Tanaka, H., Hori, O., Ogawa, S., Stern, D. M., and Schmidt, A. M. Blockade of RAGE-amphoterin signaling suppresses tumour growth and metastases. Nature (Lond.), *405:* 354–360, 2000.
20. Miettinen, M., Sarlomo-Rikala, M., Sobin, L. H., and Lasota, J. Gastrointestinal stromal tumors and leiomyosarcomas in the colon. Am. J. Surg. Pathol., *24:* 1339–1352, 2000.
21. Timeus, F., Crescenzio, N., Valle, P., Pistamiglio, P., Piglione, M., Garelli, E., Ricotti, E., Rocchi, P., Strippoli, P., Cordero di Montezemolo, L., Madon, E., Ramenghi, U., and Basso, G. Stem cell factor suppresses apoptosis in neuroblastoma cell lines. Exp. Hematol., *25:* 1253–1260, 1997.
22. Hines, S. J., Litz, J. S., and Krystal, G. W. Coexpression of c-kit and stem cell factor in breast cancer results in enhanced sensitivity to members of the EGF family of growth factors. Breast Cancer Res. Treat., *58:* 1–10, 1999.
23. Simak, R., Capodieci, P., Cohen, D. W., Fair, W. R., Scher, H., Melamed, J., Drobnjak, M., Heston, W. D., Stix, U., Steiner, G., and Cordon-Cardo, C. Expression of c-kit and kit-ligand in benign and malignant prostatic tissues. Histol. Histopathol., *15:* 365–374, 2000.
24. Bellone, G., Carbone, A., Sibona, N., Bosco, O., Tibaudi, D., Smirne, C., Martone, T., Gramigni, C., Camandona, M., Emanuelli, G., and Rodeck, U. Aberrant activation of c-kit protects colon carcinoma cells against apoptosis and enhances their invasive potential. Cancer Res., *61:* 2200–2206, 2001.
25. Flohr, A. M., Rogalla, P., Meiboom, M., Borrmann, L., Krohn, M., Thode-Halle, B., and Bullerdiek, J. Variation of HMGB1 expression in breast cancer. Anticancer Res., *21:* 3881–3885, 2001.
26. Xiang, Y. Y., Wang, D. Y., Tanaka, M., Suzuki, M., Kiyokawa, E., Igarashi, H., Naito, Y., Shen, Q., and Sugimura, H. Expression of high-mobility group-1 mRNA in human gastrointestinal adenocarcinoma and corresponding non-cancerous mucosa. Int. J. Cancer, *74:* 1–6, 1997.
27. Kawahara, N., Tanaka, T., Yokomizo, A., Nanri, H., Ono, M., Wada, M., Kohno, K., Takenaka, K., Sugimachi, K., and Kuwano, M. Enhanced coexpression of thioredoxin and high mobility group protein 1 genes in human hepatocellular carcinoma and the possible association with decreased sensitivity to cisplatin. Cancer Res., *56:* 5330–5333, 1996.
28. Chu, G., and Chang, E. Cisplatin-resistant cells express increased levels of a factor that recognizes damaged DNA. Proc. Natl. Acad. Sci. USA, *87:* 3324–3328, 1990.
29. Chu, G. Cellular responses to cisplatin. The roles of DNA-binding proteins and DNA repair. J. Biol. Chem., *269:* 787–790, 1994.
30. Bustin, M. Regulation of DNA-dependent activities by the functional motifs of the high-mobility-group chromosomal proteins. Mol. Cell. Biol., *19:* 5237–5246, 1999.
31. Passalacqua, M., Zicca, A., Sparatore, B., Patrone, M., Melloni, E., and Pontremoli, S. Secretion and binding of HMG1 protein to the external surface of the membrane are required for murine erythroleukemia cell differentiation. FEBS Lett., *400:* 275–279, 1997.
32. Wang, H., Bloom, O., Zhang, M., Vishnubhakat, J. M., Ombrellino, M., Che, J., Frazier, A., Yang, H., Ivanova, S., Borovikova, L., Manogue, K. R., Faist, E., Abraham, E., Andersson, J., Andersson, U., and Molina, P. E., Abumrad, N. N., Sama, A., and Tracey, K. J. HMG-1 as a late mediator of endotoxin lethality in mice. Science (Wash. DC), *285:* 248–251, 1999.
33. Muller, S., Scaffidi, P., Degryse, B., Bonaldi, T., Ronfani, L., Agresti, A., Beltrame, M., and Bianchi, M. E. New EMBO members' review: the double life of HMGB1 chromatin protein: architectural factor and extracellular signal. EMBO J., *20:* 4337–4340, 2001.
34. Bianchi, M. E., and Beltrame, M. Upwardly mobile proteins. The role of HMG proteins in chromatin structure, gene expression and neoplasia. EMBO Rep., *1:* 109–119, 2000.
35. Stros, M., Ozaki, T., Bacikova, A., Kageyama, H., and Nakagawara, A. HMGB1 and HMGB2 cell-specifically down-regulate the p53- and p73-dependent sequence-specific transactivation from the human *Bax* gene promoter. J. Biol. Chem., *277:* 7157–7164, 2002.